VILNIUS TECH
Vilnius Gediminas
Technical University

Civil engineering
Statybos inžinerija

FEM ANALYSIS OF ENERGY LOSS DUE TO WAVE PROPAGATION FOR MICRO-PARTICLE IMPACTING SUBSTRATE WITH HIGH VELOCITIES

Giedrius JOČBALIS [ID] *

Vilnius Gediminas Technical University, Vilnius, Lithuania

Abstract. The impact between particles and material surface is a micro-scaled physical phenomenon found in various technological processes and in the study of the mechanical properties of materials. Design of materials with desired properties is a challenging issue for most industries. And especially in aviation one of the most important factors is mass. Recently with the innovations in 3D printing technologies, the importance of this phenomenon has increased. Numerical simulation of multi-particle systems is based on considering binary interactions; therefore, a simplified but as much accurate as possible particle interaction model is required for simulations.

Particular cases of axisymmetric particle to substrate contact is modelled at select impact velocities and using different layer thicknesses. When modelling the particle impact at high contact velocity, a substrate thickness dependent change in the restitution coefficient was observed. This change happens is due to elastic waves and is important both to coating and 3D printing technologies when building layers of different properties materials.

Keywords: particle-wall interaction, substrate thickness, perfectly elastic collision, high velocity contact, normal contact, elastic waves, coefficient of restitution.

Introduction

Motivation. Design of materials with desired properties is a challenging issue for most industries. Reduction of the relative mass compared to strength is specifically required in aerospace engineering. Recent developments of three-dimensional (3D) printing technology (Bae et al., 2018) allow manufacture of material having specified material structure on microscale and final products shaped by much more complex topology on macroscale. Current Laser Melted Deposition (LMD) technology allows the latter by supplying metal particles only to the printing location (melting pool). In Cold spray metal coating technology, the local melting temperature is generated from the energy of the particle impact. Therefore, by examining the specifics of the particle-surface interactions and applying the particle delivery principle used in cold spray technologies, the printing resolution can be further increased.

The impact of a particle on a material surface is a physical phenomenon found in various technological processes and in the study of the mechanical properties of materials. Settling of microparticles on the substrate is important technological operation required in production of material. Flow and transfer of the energy during particle-substrate impact plays decisive role for post-impact behavior and properties of material. Kinetic energy of moving particle is transferred to substrate, and a part of it is dissipated through various dissipation mechanisms. Loss of energy during impact because of propagation of elastic waves is one of those mechanisms.

The earlier research of dissipation related to wave propagation was limited to low-velocity impact of millimeter sized particles. Generally, this effect is negligibly small for interacting particles. When impacting massive body, its contribution reaches even several percent (Seifried et al., 2005). Its significance is basically observed in the beginning of elastic contact (Weir & Tallon, 2005). Short impulse force effect on large plates is investigated by (Zener, 1941) and gives basis for sphere to large plate contact theories. Latest results on the elastic wave dissipation mechanism (Boettcher et al., 2017a) and its combination with visco-elastic deformation, are limited to low velocity impact and was demonstrated in Aman et al. (2016) and Boettcher et al. (2019). Technology of the 3D printing operates, however, with high velocity, up to 500 m/s

*Corresponding author. E-mail: *giedrius.jocbalis@vilniustech.lt*

impacts of micron-sized particles of diameter ranging between 1 and 300 microns. High velocity contact is usually modelled using Johnson-cook strain rate dependent yield criterion and is demonstrated by Yokoyama et al. (2006) and Wang et al. (2015).

The main focus of this article is investigation of loss of energy during particle-substrate interaction. For this purpose, Hertz normal contact model was considered as a base-line and only perfectly elastic axisymmetric particle to substrate contact is modelled at select impact velocities and using different layer thicknesses. When modelling the particle impact at high contact velocity, a substrate thickness dependent change in the restitution coefficient was observed. This change happens due to elastic waves and is important both to coating and 3D printing technologies when building layers of different properties materials.

1. Problem formulation

Normal impact addressed hereafter is formulated in the following manner. The smooth spherical particle of radius R_p = 20 μm represent common size powder particle, the substrate represents infinite layer of thickness H that ranges from 5 to 1000 μm.

Shown in Figure 1. a) particle approaching surface, its velocity is affected by air flow and resistance, b) time instance of contact, particle reaches surface with initial contact velocity v_0, c) maximum contact depth $d = d_{max}$, both particle and substrate deforms, particle velocity $v = 0$ m/s, elastic waves propagate d) particle rebounds with rebound velocity v_r elastic waves continue propagating in substrate.

Smooth spherical particle colliding with smooth horizontal surface of the substrate is characterized by one-dimensional (1D) motion of colliding partners in normal direction.

The density ρ and two elastic constants (elasticity modulus E and Poissons ratio ν) are the most important primary parameters. The secondary parameters shear modulus G and elastic wave velocities are obtained by Eq. (1–4) the data set of copper used in our analysis is presented in Table 1.

Here shear modulus is related to Young modulus through

$$G = \frac{E}{2(1+\nu)}, \tag{1}$$

compression, shear and Rayleigh wave velocities calculated using following equations (Weir & Tallon, 2005) compression wave velocity:

Table 1. Basic parameters of particle and substrate layer

Parameter	Notation	Unit	Value
Young modulus	E	GPa	128
Poissons coefficient	ν	1	0.36
Shear modulus	G	GPa	47.059
Density	ρ	kg/m³	8960
Compression wave velocity	c_p	m/s	4899.969
Shear wave velocity	c_s	m/s	2291.746
Surface (Rayleigh) wave velocity	c_R	m/s	2154.241

$$c_p = \sqrt{\frac{2(1-\nu)G}{(1-2\nu)\rho}}, \tag{2}$$

shear wave velocity:

$$c_s = \sqrt{\frac{G}{\rho}}, \tag{3}$$

surface wave velocity:

$$c_R = 0.94 c_s. \tag{4}$$

Figure 2 shows modelled substrate boundary conditions as a) base – representing a plate on top of material with extremely high Young modulus, and b) plate – representing free thin plates or a layer on top of material with much lower Young modulus. In this article computing results are given using substrate base, while plate model is only used to compare to Zener model (Zener, 1941; Aman et al., 2016; Müller et al., 2016; Xd & Xd, 2017).

The impacts at different layer thickness – H are solved by the finite element analysis, using COMSOL Multiphysics FEA software dynamic solver, governing equation:

$$\rho \frac{\partial^2 u}{\partial t^2} = \nabla \cdot (F\,S)^{\mathrm{T}} + F_V. \tag{5}$$

Due to axial symmetry of normal contact, the two-dimensional axisymmetric space dimension will be applied. The finite radius of plate R is selected to fulfill requirements for infinite layer $R \gg R_p$ and $R > H$ (Figure 3).

Boundary conditions applied for modeled substrate external perimeter

$$u \cdot n = 0 \tag{6}$$

and substrate bottom surface

$$u = 0 \tag{7}$$

in case of substrate plate, boundary condition for substrate bottom surface does not apply (Figure 2).
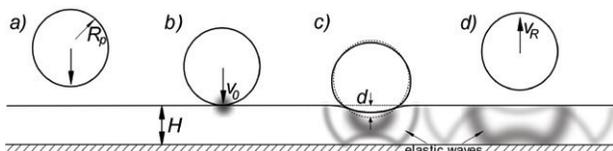

Figure 1. Schematic illustration of particle – substrate interaction stages: a) particle approach, b) time instance of contact, c) maximum contact depth, d) rebound
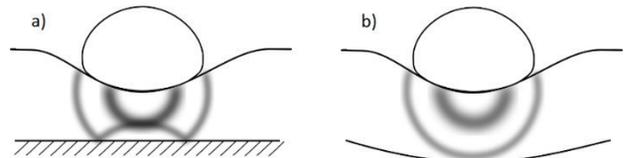

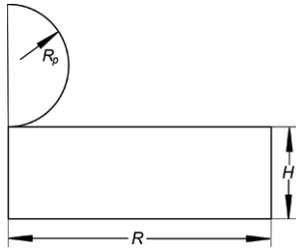Figure 2. Substrate modeling conditions: a) base, b) plate
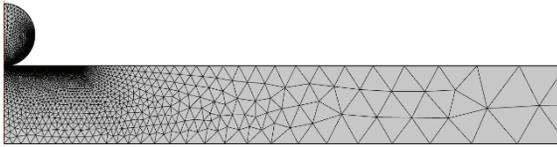
Figure 3. Finite element model schematics

Figure 4. Finite element model mesh used for calculations

Contact is formulated by penalty function

$$T_n = \mathrm{if}\left(g_n \le 0, -p_n g_n, 0\right), \tag{8}$$

where g_n is distance between contact surfaces and p_n – penalty factor defined by characteristic stiffness Echar through

$$p_n = \frac{E_{char}}{h_{min}}. \tag{9}$$

As initial values impact velocities used are: 2, 20, 200 and 500 m/s.

Optimized meshes used for different substrate thickness calculations are denser at contact point and are made of 3.5k to 4.5k elements (Figure 4). And meshes used for wave propagation investigation are more uniform and has 15k and 32k elements.

The initial conditions are as follows:

$$\delta(0) = 0 \text{ and } \dot{\delta}(0) = v_0. \tag{10}$$

2. Computational results

Using calculated elastic wave velocities (in Table 1) these waves can be identified in pressure and energy density (Figure 5 and Figure 6) graphs.

The images at the top (Figure 5) show energy density of thin base substrate in the beginning of contact (a) we can see elastic wave starting to propagate through substrate in radial manner, deepest point of contact (c) shear wave returns from the bottom of substrate base increasing restitution force, at the moment of separation (e) and after the separation (g), graphs on the left (b, d, f and h) shows corresponding energy density across radius of the substrate mid-layer. The velocity of observed wave is equal to calculated elastic shear wave velocity.

Figure 6a shows pressure distribution after 500 m/s contact in model cross-section. In this case compression wave can be seen as pressure front. Thin lines show expected compression and shear wave positions at current frame calculated using wave velocities. In this case compression wave can be seen as pressure front.
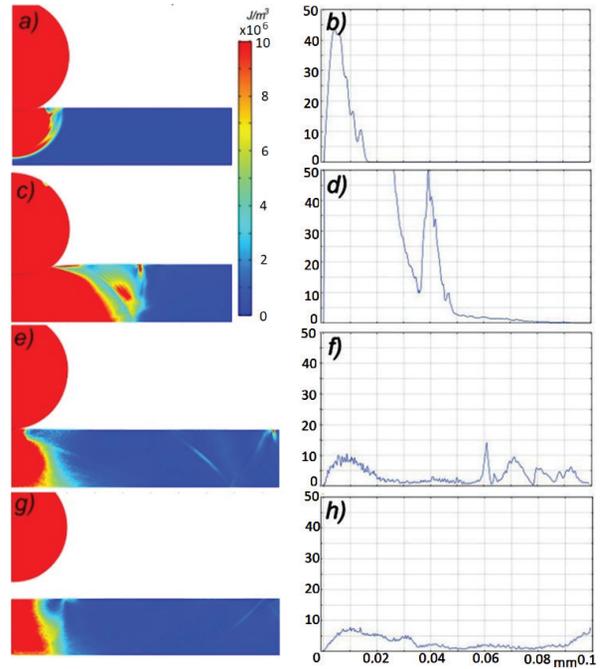

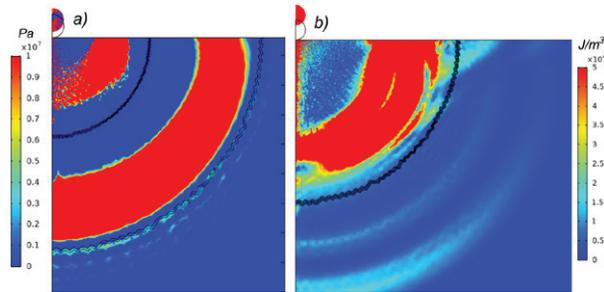Figure 5. Elastic shear wave shown by energy density graphs

Figure 6. Elastic compression wave shown by pressure graph on the left, energy density graph on the right

Integrating energy across volume of substrate where elastic waves are expected to be at given time moment, we get energy distribution: around 10% of energy lost by particle is contained by compression wave, while other 90% is contained by slower shear and surface waves. Separation line used for wave energy integration is shown in Figure 6b.

2.1. Contact depth and velocity

In the case of contacting surfaces, normalization could be procured by applying the Hertz solution (Luding et al., 1994) and introducing the time scaling parameter:

$$T = \left(\frac{5}{4}\frac{m}{K_H}\right)^{\frac{2}{5}} v_0^{-\frac{1}{5}}, \tag{11}$$

where the effective constant K_H is defined by

$$K_H = \frac{4}{3} E_{eff} \sqrt{R}, \tag{12}$$

where R – sphere radius, E_{eff} – effective Young modulus defined as

$$E_{eff} = \frac{E}{2(1-v^2)}. \qquad (13)$$

The duration of the Hertz contact and maximal indentation are defined by expressions:

$$T_{Hertz} = 2.94T, \qquad (14)$$

$$\delta_{Hertz} = Tv_0. \qquad (15)$$

For Hertz model, time step integration code of normal Hertz force was written.

$$F_H = \frac{4}{3} E_{eff} \sqrt{R} \sqrt{d^3}, \qquad (16)$$

where: F_H – Hertz normal force, d – contact depth.

Contact depth and particle velocity from FEM models are obtained by calculating average displacement and velocity of particle volume. FEM results for different substrate thickness as well as results obtained from Hertz model are shown in Figure 7.

From the Figure 7 graphs we can see that at the lower impact speed the influence of the base thickness is smaller and stops increasing only at the base thickness around 250 μm. At higher velocities of 200 and 500 m/s, the influence of the substrate thickness is higher and stops increasing when the substrate is between 50 and 100 μm thick. It can be seen from all these graphs that the thinner modeled base behaves similar to a material with higher stiffness, the lesser contact time and depth are obtained due to the higher restitution force.

Also, at lower particle velocities the restitution coefficient remains close to 1 and only the change in contact duration is visible. Restitution coefficient changes minimally, it decreases equally at the base 150 μm and higher. At higher impact velocities, a sharp decrease in the restitution coefficient is observed at a base thickness between 20 and 100 μm.

2.2. Contact duration

Contact time for substrate base FEM models is considered a time when average particle volume displacement returns to zero. Contact duration dependence on substrate thickness at different impact velocities is shown in Figure 8.

In Figure 8 we can see that contact duration is shorter for thinner base models and becomes constant when increasing base thickness.
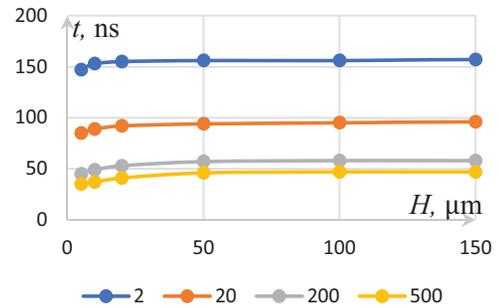

Figure 8. Particle-substrate contact duration dependency on substrate thickness at different impact velocities
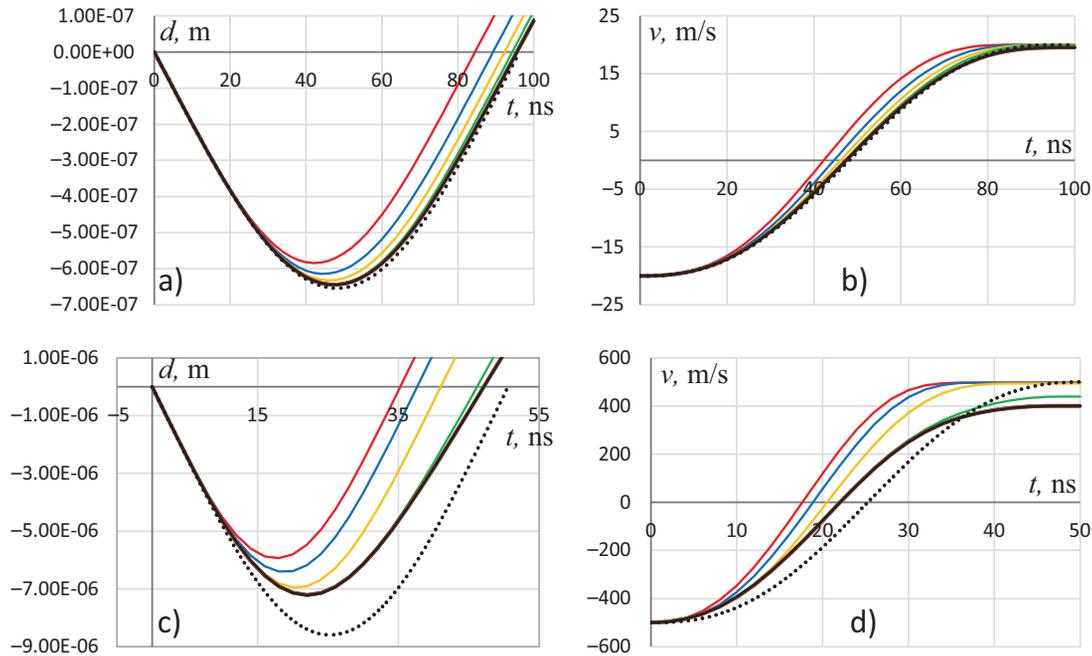

Figure 7. Contact depth and velocity graphs (graphs of depth and velocity during 20 m/s impact are shown in figures a and b, respectively, and graphs of impact with an initial velocity of 500 m/s are presented in figures c and d. Substrate thicknesses red – 5 μm, blue – 10 μm, yellow – 20 μm, green – 50 μm, thickness of 100 μm to 1000 μm are identical and marked in black, Hertz model results shown in black dotted line)

4

2.3. Coefficient of restitution

In thin substrates elastic wave propagates during contact causing either reflected wave or plate deformation that leads to higher or lower COR respectively.

When substrate is thin and contact time is longer than wave propagation time two things may occur:

1. If substrate layer is on top of harder surface elastic wave rebounds therefore increasing COR;
2. If substrate layer is on top of softer surface elastic wave deforms the plate therefore further decreasing COR.

For these extreme cases substrate is modelled as base and plate (shown in Figure 2).
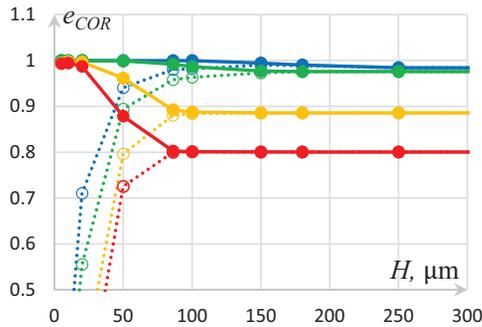

Figure 9. Dependence of the restitution coefficient on the thickness of the modelled base at different impact velocities blue – 2 m/s, green – 20 m/s, yellow 200 m/s and red 500 m/s dotted lines show restitution coefficient obtained using substrate plate model

In the diagram we see the value of restitution coefficient dependency on modeled surface thickness. In this case we see that at 500 m/s impact velocity coefficient of restitution is around 0.8 and surface thickness of 5R (5 particle radii) is sufficient for model

3. Discussion

The graphs in Figure 9 the values of the base thickness at which the restitution coefficient stops decreasing can be seen. These values roughly correspond to the distance elastic wave travels during the second half of the contact.

$$d(v) = \frac{cT(v)}{2}, \tag{17}$$

where $d(v)$ – distance the wave travels, c – wave propagation velocity, $T(v)$ – contact time.

Otherwise comparable to elastic wave propagation time (Aman et al., 2016)

$$t_{prop} = \frac{2H}{c}, \tag{18}$$

where t_{prop} – elastic wave propagation time, H – plate thickness.

Plate thickness influence on COR at low velocities is demonstrated by (Zener, 1941). Inelasticity coefficient is calculated using (Zener, 1941) equations also used by (Aman et al., 2016; Xd & Xd, 2017; Boettcher et al., 2017b).

$$\lambda = \frac{\pi^{3/5}}{\sqrt{3}} \left(\frac{R_1}{2h_p} \right)^2 \left(\frac{v_a}{c} \right)^{1/5} \left(\frac{\rho_1}{\rho_2} \right)^{3/5} \left(\frac{E_1 / (1 - \mu_1^2)}{E_1 / (1 - \mu_1^2) + E_2 / (1 - \mu_2^2)} \right)^{2/5}. \tag{19}$$

When particle and surface is made of the same material simplified equation can be used

$$\lambda = \frac{\pi^{3/5}}{\sqrt{3}} \left(\frac{R_1}{2h_p} \right)^2 \left(\frac{v_a}{4c} \right)^{1/5}, \tag{20}$$

where λ – inelasticity coefficient, R_1 – particle radius, h_p – half of plate thickness, v_a – initial particle velocity, c – wave propagation velocity

Figure 10. Coefficient of restitution for 2 m/s impact comparison between Zener model and FEM model (blue line finite element model with substrate plate, dotted line Zener model)
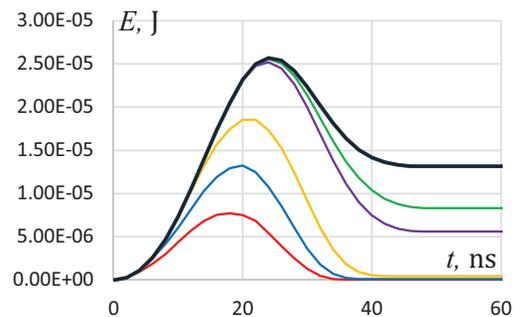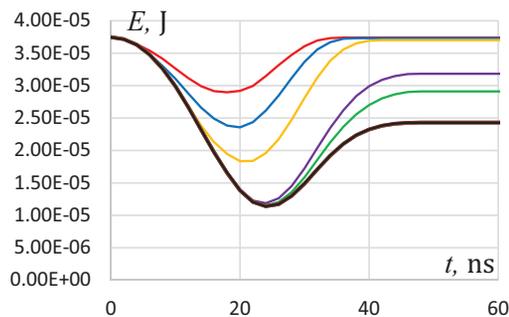

Figure 11. Particle and substrate energy during impact (particle energy at 500 m/s contact is shown on the left, substrate energy during same contact on the left. Substrate thicknesses red – 5 μm, blue – 10 μm, yellow – 20 μm, green – 50 μm, thickness of 100 μm to 1000 μm marked in black)

Zener model comparison with impact velocity 2 m/s finite element substrate plate model is shown in Figure 10.

Coefficient of restitution used to illustrate Zener model is related to inelasticity coefficient through (Boettcher et al., 2017b) approximation

$$e_{COR} = \exp\left(-1{,}7174\lambda\right). \tag{21}$$

From Figure 10 we can see that at low velocities coefficient of restitution calculated using finite element substrate plate model is slightly smaller than obtained by Zener model. Adding to that results in Figure 9, predictions can be made that at lowest impact velocities FEM and Zener models would yield same results.

From the energy graphs of the particle and the substrate (Figure 11), we can see that the amount of energy delivered to the substrate by the particle stops increasing at a certain substrate thickness and the particle does not recover the initial energy.

Conclusions

The study of energy dissipation leads to the following conclusions:

Substrate thickness influences the value of coefficient of restitution due to elastic wave propagation.

Using thinner base model, we get smaller contact depth, shorter impact time, higher COR and less energy is transferred from particle to base. In case of thin plate, effect is opposite – contact is deeper, contact time is longer, lower COR, and more kinetic energy is transferred from particle to plate. While investigation of models with thicker base and plate yields identical results.

In thicker substrate about 10% of energy lost by particle is contained by compression wave, while other 90% is contained by slower shear and surface waves.

At low particle velocities for modeling particle – plate interaction Zener model is sufficient.

Acknowledgements

References

Aman, S., Mueller, P., Tomas, J., Kozhar, S., Dosta, M., & Heinrich, S. (2016). Combined viscoelastic and elastic wave dissipation mechanism at low velocity impact. *Advanced Powder Technology*, 27(4), 1244–1250. https://doi.org/10.1016/j.apt.2016.04.012

Bae, C.-J., Diggs, A. B., & Ramachandran, A. (2018). 6 – Quantification and certification of additive manufacturing materials and processes. In J. Zhang & Y.-G. Jung (Eds.), *Additive manufacturing: Materials, processes, quantifications and applications*. Elsevier. https://doi.org/https://doi.org/10.1016/b978-0-12-812155-9.00006-2

Boettcher, R., Eichmann, S., & Mueller, P. (2019). Influence of viscous damping and elastic waves on energy dissipation during impacts. *Chemical Engineering Science*, 199, 571–587. https://doi.org/10.1016/j.ces.2019.01.036

Boettcher, R., Kunik, M., Eichmann, S., Russell, A., & Mueller, P. (2017a). Revisiting energy dissipation due to elastic waves at impact of spheres on large thick plates. *International Journal of Impact Engineering*, 104, 45–54. https://doi.org/10.1016/j.ijimpeng.2017.02.012

Boettcher, R., Russell, A., & Mueller, P. (2017b). Energy dissipation during impacts of spheres on plates: Investigation of developing elastic flexural waves. *International Journal of Solids and Structures*, 106–107, 229–239. https://doi.org/10.1016/j.ijsolstr.2016.11.016

Luding, S., Clément, E., Blumen, A., Rajchenbach, J., & Duran, J. (1994). Anomalous energy dissipation in molecular-dynamics simulations of grains: The "detachment" effect. *Physical Review E*, 50(5), 4113–4122. https://doi.org/10.1103/PhysRevE.50.4113

Müller, P., Böttcher, R., Russell, A., Trüe, M., Aman, S., & Tomas, J. (2016). Contact time at impact of spheres on large thin plates. *Advanced Powder Technology*, 27(4), 1233–1243. https://doi.org/10.1016/j.apt.2016.04.011

Seifried, R., Schiehlen, W., & Eberhard, P. (2005). Numerical and experimental evaluation of the coefficient of restitution for repeated impacts. *International Journal of Impact Engineering*, 32(1–4), 508–524. https://doi.org/10.1016/j.ijimpeng.2005.01.001

Wang, X., Feng, F., Klecka, M. A., Mordasky, M. D., Garofano, J. K., El-Wardany, T., Nardi, A., & Champagne, V. K. (2015). Characterization and modeling of the bonding process in cold spray additive manufacturing. *Additive Manufacturing*, 8, 149–162. https://doi.org/10.1016/j.addma.2015.03.006

Weir, G., & Tallon, S. (2005). The coefficient of restitution for normal incident, low velocity particle impacts. *Chemical Engineering Science*, 60, 3637–3647. https://doi.org/10.1016/j.ces.2005.01.040

Xd, T. X., & Xd, D. X. (2017). A size-dependent viscoelastic normal contact model for particle collision. *International Journal of Impact Engineering*, 106, 120–132. https://doi.org/10.1016/j.ijimpeng.2017.03.020

Yokoyama, K., Watanabe, M., Kuroda, S., Gotoh, Y., Schmidt, T., & Gärtner, F. (2006). Simulation of solid particle impact behavior for spray processes. *Materials Transactions*, 47(7), 1697–1702. https://doi.org/10.2320/matertrans.47.1697

Zener, C. (1941). The intrinsic inelasticity of large plates. *Physical Review*, 59(8), 669–673. https://doi.org/10.1103/PhysRev.59.669

Notations

Abbreviations

COR – Coefficient of restitution;
FEA – Finite element analysis;
FEM – Finite element method.

MIKRODALELĖS, SMOGIANČIOS Į PAGRINDĄ DIDELIU GREIČIU, ENERGIJOS NUOSTOLIO DĖL BANGŲ SKLIDIMO BEM ANALIZĖ

G. Jočbalis

Santrauka

Smūgis tarp dalelių ir medžiagos paviršiaus yra mikromasto fizikinis reiškinys, aptinkamas įvairiuose technologiniuose

procesuose ir tiriant medžiagų mechanines savybes. Norimų savybių medžiagų projektavimas yra sudėtingas uždavinys daugelyje pramonės šakų. Aviacijoje ypač svarbus faktorius yra masė. Pastaruoju metu tobulėjant 3D spausdinimo technologijoms šio reiškinio svarba išauga. Daugiadalelinių sistemų skaitinis modeliavimas pagrįstas dalelių porų sąveikų vertinimu, todėl simuliacijoms reikalingas supaprastintas, bet kuo tikslesnis dalelių sąveikos modelis.

Šiame darbe nagrinėjami keli dalelių ir pagrindo kontakto atvejai tarp skirtingu greičiu judančios dalelės ir skirtingo storio pagrindo. Modeliuojant dalelės ir pagrindo sąveiką, esant dideliam kontakto greičiui, buvo pastebėtas nuo pagrindo storio priklausomas restitucijos koeficiento pokytis. Šis pokytis atsiranda dėl tampriųjų bangų ir yra svarbus tiek medžiagos padengimo, tiek 3D spausdinimo technologijoms kaupiantis skirtingų savybių medžiagų sluoksniams.

Reikšminiai žodžiai: dalelės ir sienos sąveika, pagrindo storis, visiškai tamprus smūgis, didelio greičio kontaktas, normalinis kontaktas, tampriosios bangos, restitucijos koeficientas.